Low Loss EELS

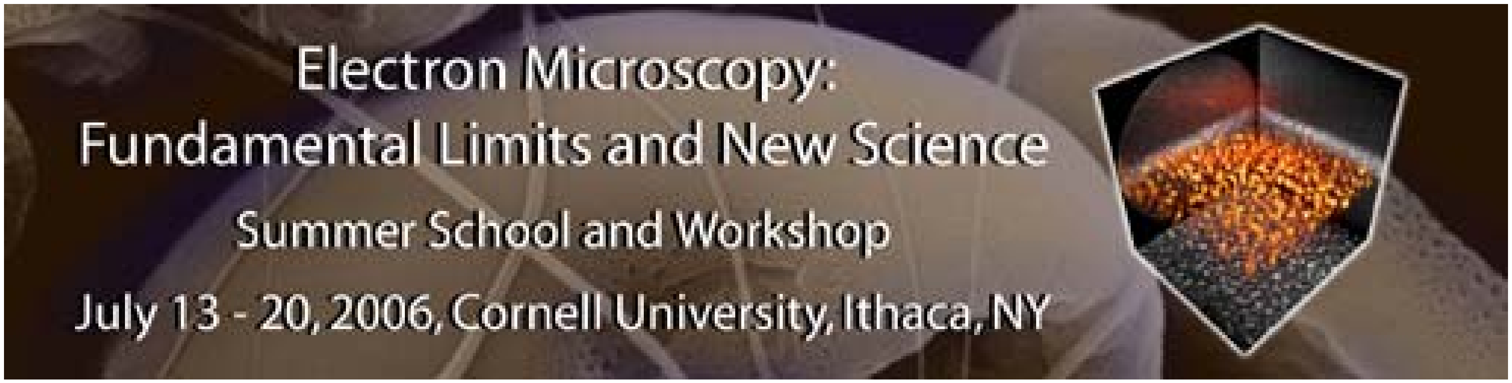

Notes to accompany the lectures delivered by David A. Muller at the Summer School on Electron Microscopy: Fundamental Limits and New Science held at Cornell University, July 13-15, 2006.

Additional Reading and References:

Kohl & Rose, *Adv. Electron. Electron Phys*. **65** (1985) 173.
Muller & Silcox, *Ultramicroscopy* **59** (1995) 195.

How Delocalized is an EELS Signal?

For E_0=100 keV electrons, λ=0.037 Å, v=1.64x10^8 m/s

For dipole scattering, the cross section is $\frac{d^2\sigma}{d\Omega dE} \;\alpha\; \frac{1}{\theta^2+\theta_E^2}\left|\left\langle f\left|r\right|i\right\rangle\right|^2\rho_f(\Delta E)$

with the characteristic angle at energy loss ΔE of $\theta_E \equiv \frac{\Delta E}{2E_0}$

By analogy with the Raleigh resolution criterion, we might expect a resolution of

$$r_{inel} \approx \frac{\lambda}{\theta_E}$$

(this would assume that all the scattering lies inside θ_E, which is not true).

For an energy loss ΔE=20 eV, we get $r_{inel} = 6.5\,nm$

How Delocalized is an EELS Signal?

Diamond Nanoparticle in ZnS

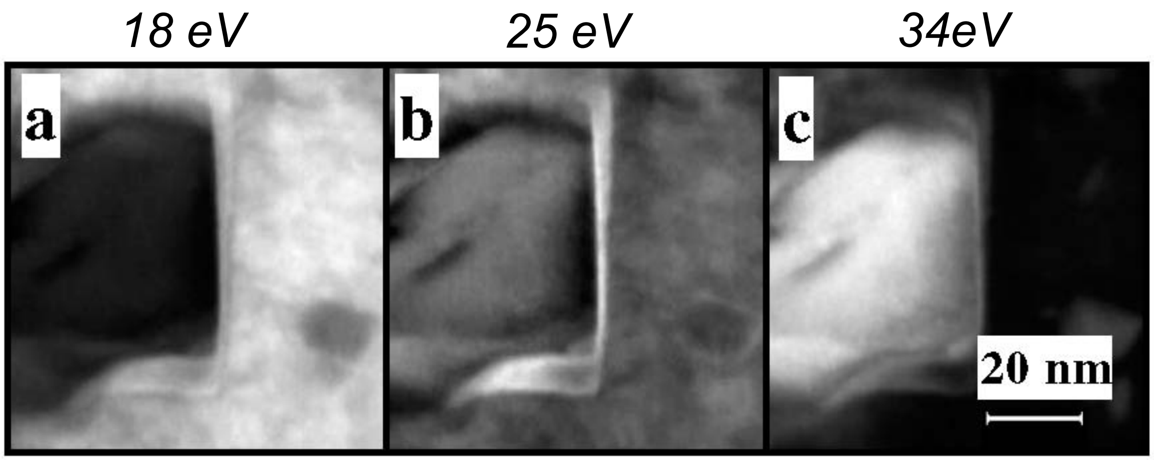

Muller & Silcox, *Ultramicroscopy* **59** (1995) 195.

An upper limit to the cutoff angle is the maximum momentum transfer in the small-angle approximation. This is also the peak of the Bethe Ridge at

$$\theta_B \approx \sqrt{2\theta_E}$$

Which gives

$$r_{\min} \approx \lambda \sqrt{\frac{E_0}{\Delta E}}$$

or 0.26 nm for ΔE=20 eV which is a little too small.

The real answer seems to lie between r_{inel} and r_{min} (and closer to r_{min})

Dipole Theory Calculations of Inelastic Resolution

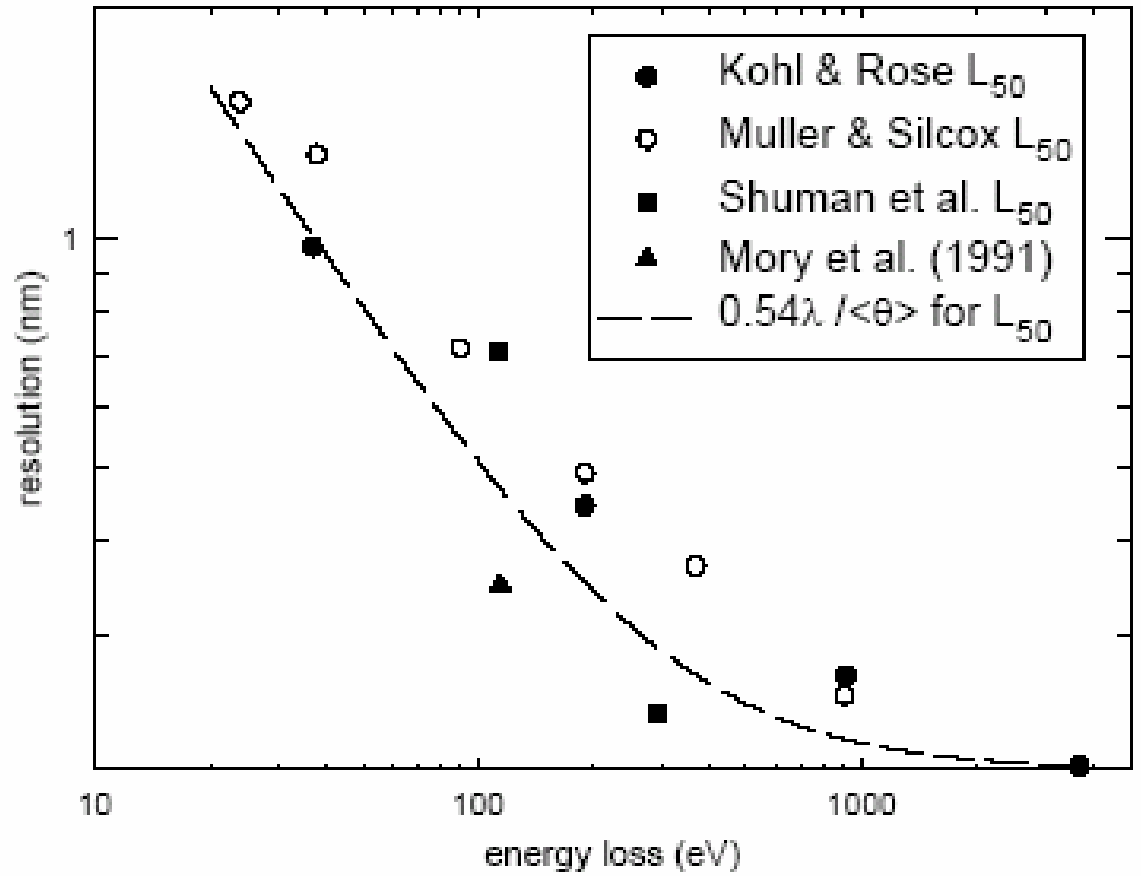

Fig.1: Localization diameter for 100keV electrons and a 10mrad on-axis detector [6].

$$\langle\theta\rangle \approx \theta_E^{3/4}$$

R. F. Egerton, *Journal of Electron Microscopy* **48** (1999) 711.

Comparison of Dipole and Full Atomic Calculations

For a free atom, agreement is ~10% or better.
Crystal channeling could cause problems

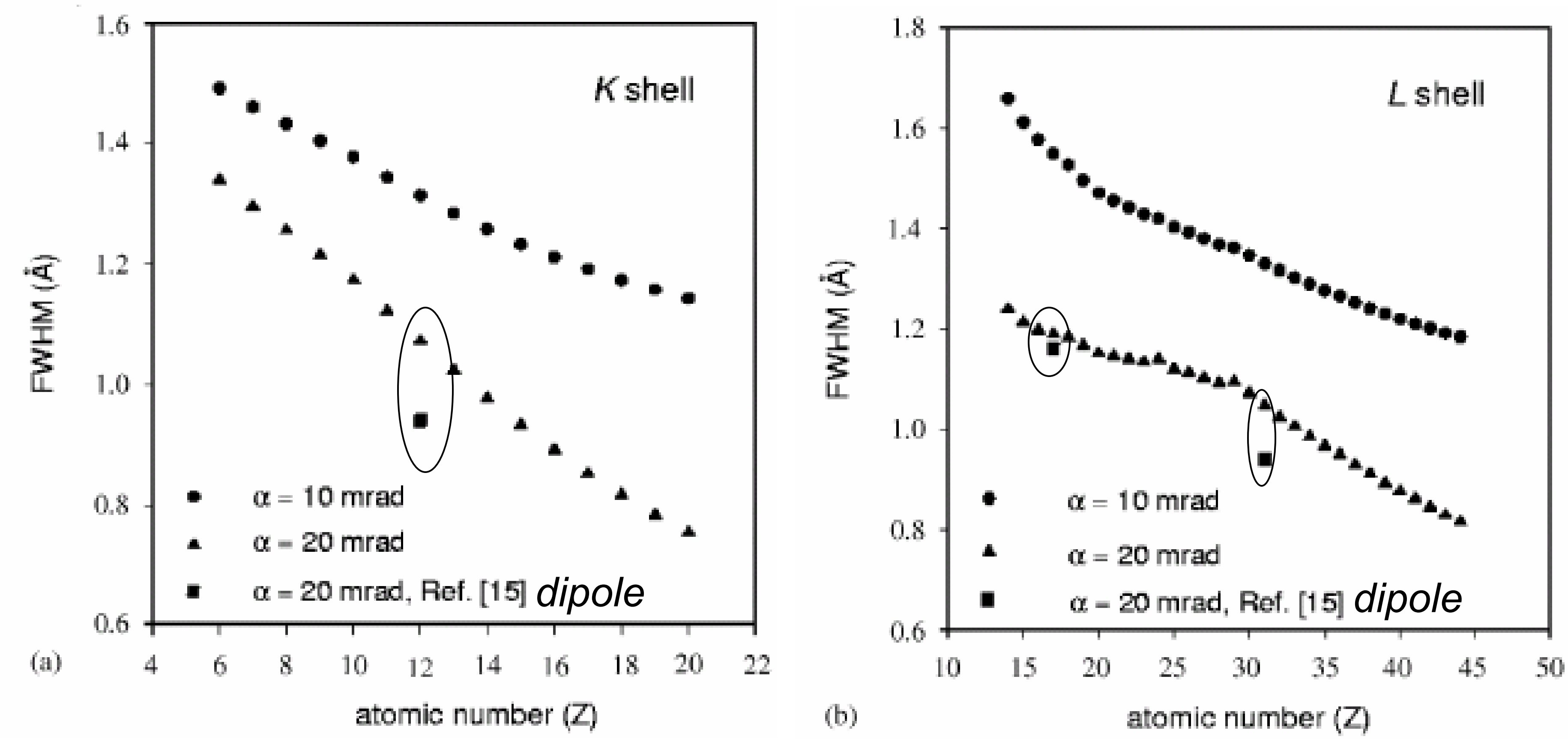

E.C. Cosgriff et al. / Ultramicroscopy 102 (2005) 317–326

Classical Picture of Energy Loss by a Fast, Charged Particle (Bohr, 1913)

Consider a fast e- that passes a free, target charge and is deflected through a small angle

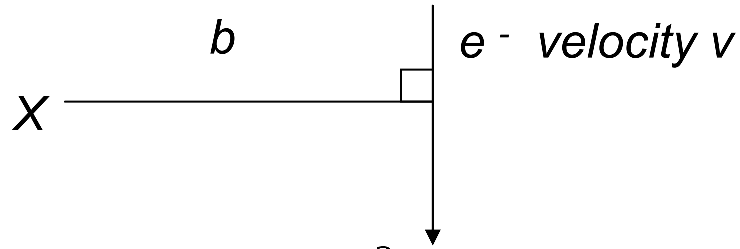

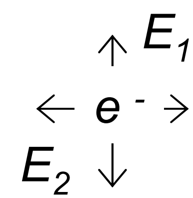

Dipole field

Momentum transfer $\Delta p = \int_{-\infty}^{\infty} e\, E_2(t)\, dt = \dfrac{2e^2}{bv}$

Energy Loss $\Delta E(b) = \dfrac{(\Delta p)^2}{2m} = \dfrac{2e^4}{mv^2}\dfrac{1}{b^2}$

Energy loss is a function of impact parameter

Quantum Treatment (Single scattering, linear imaging)

For a probe wavefunction a(b) , detector function D and transmission function w(x,x',E)
The probability of losing energy E at distance b from the atom is

$$P(b, E) = \frac{4R_y}{E_0} \int a(\boldsymbol{\rho} - \boldsymbol{b}) a^*(\boldsymbol{\rho}' - \boldsymbol{b}) \times w(\boldsymbol{\rho}, \boldsymbol{\rho}', E) D(\boldsymbol{\rho} - \boldsymbol{\rho}') \, \mathrm{d}^2\boldsymbol{\rho} \, \mathrm{d}^2\boldsymbol{\rho}'.$$

The detector controls overlap of the wavefunction from different positions in the sampl
i.e. it controls the coherence volume (optics) or degree of nonlocality of the probe (QM

For a tiny aperture on axis, $D(\boldsymbol{\rho} - \boldsymbol{\rho}') = \frac{2\pi\beta_0^2 J_1(k\beta_0 |\boldsymbol{\rho} - \boldsymbol{\rho}'|)}{k\beta_0 |\boldsymbol{\rho} - \boldsymbol{\rho}'|} \rightarrow \pi\beta_0^2,$

which allows coherence over the entire sample, i.e. a phase sensitive image

For large aperture on axis, $D(\boldsymbol{\rho} - \boldsymbol{\rho}') = \rightarrow 2\pi\beta_0^2 \delta(|\boldsymbol{\rho} - \boldsymbol{\rho}'|),$

which removes non-local overlap, i.e. an incoherent image

D.A. Muller, J. Silcox / Ultramicroscopy 59 (1995) 195–213

EELS with a Large Collector Aperture

$$P(b, E) = \frac{4R_y}{E_0} |a(b)|^2 \otimes w(\rho, \rho, E).$$

Convolution of probe intensity with response function.

$|a(b)|^2$ *has the same form as elastic incoherent imaging, but w is quite delocalized*

For a dipole excitation

$$P_D(b, E) = \frac{\beta_0^2}{\pi^2} \frac{R_y}{E_0} |a(b)|^2 \otimes \left(\frac{1}{b_{max}}\right)^2 \left[|K_0(b/b_{max}) z_{fi}|^2 + |K_1(b/b_{max}) x_{fi} \cdot \cos\gamma|^2 \right].$$

i.e. w(r,E) has the same form as the classical loss function for a dipole

D.A. Muller, J. Silcox / Ultramicroscopy 59 (1995) 195–213

EELS with a Tiny Collector Aperture

For a dipole excitation

$$P_D(b, E) = \frac{\beta_0^2}{2\pi^2}\frac{R_y}{E_0}\left(\frac{1}{b_{max}}\right)^2 \left| a(b) \otimes \left[K_0(k_0\rho\theta_E) z_{fi} + i K_1(k_0\rho\theta_E) x_{fi} \cos\gamma \right] \right|^2$$

Convolution of probe wavefunction with response function has the same form as elastic coherent imaging, but again the "inelastic object" is quite delocalized. Expect phase contrast and contrast reversals

D.A. Muller, J. Silcox / Ultramicroscopy 59 (1995) 195–213

Effect of the Collector Aperture

Donut or volcano shape

Long tails In both cases

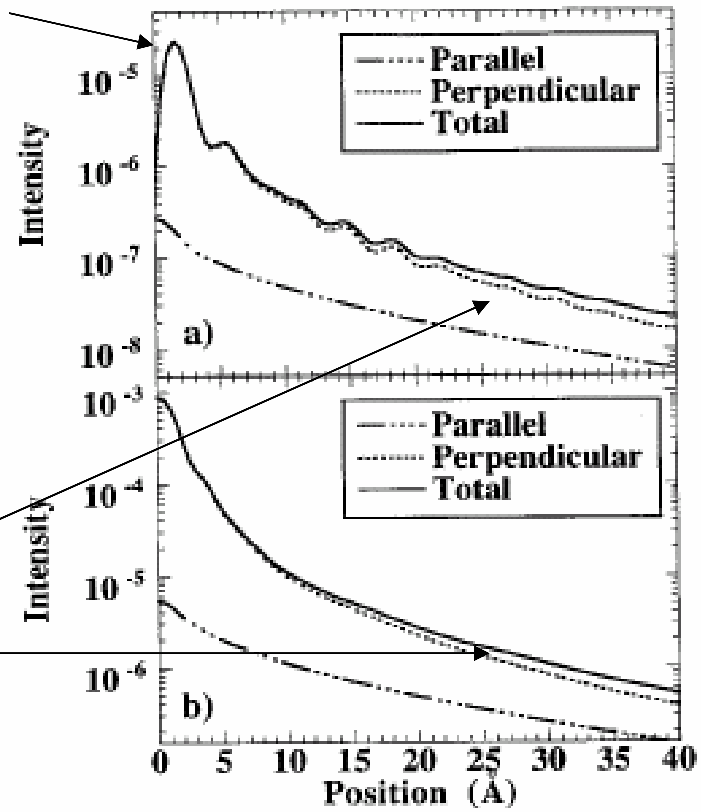

Small Collector

Large Collector

(narrower central peak)

Fig. 2. Spatial distribution of the probability for a 25 eV energy loss by a 100 keV electron beam in a STEM with $C_s = 1.3$ mm, 700 Å defocus and a 10 mrad objective aperture; (a) for a 1.6 mrad collector aperture and (b) for a 10 mrad collector aperture. The dotted line shows the component of $P(b, E)$ perpendicular to the optic axis while the dot-dashed line shows the $P(b, E)$ along the optic axis. b_{max} is at 43 Å but the semiclassical approximation holds to within 5 Å of the dipole where the "donut" shape appears.

Delocalization has long tails and a sharp central peak

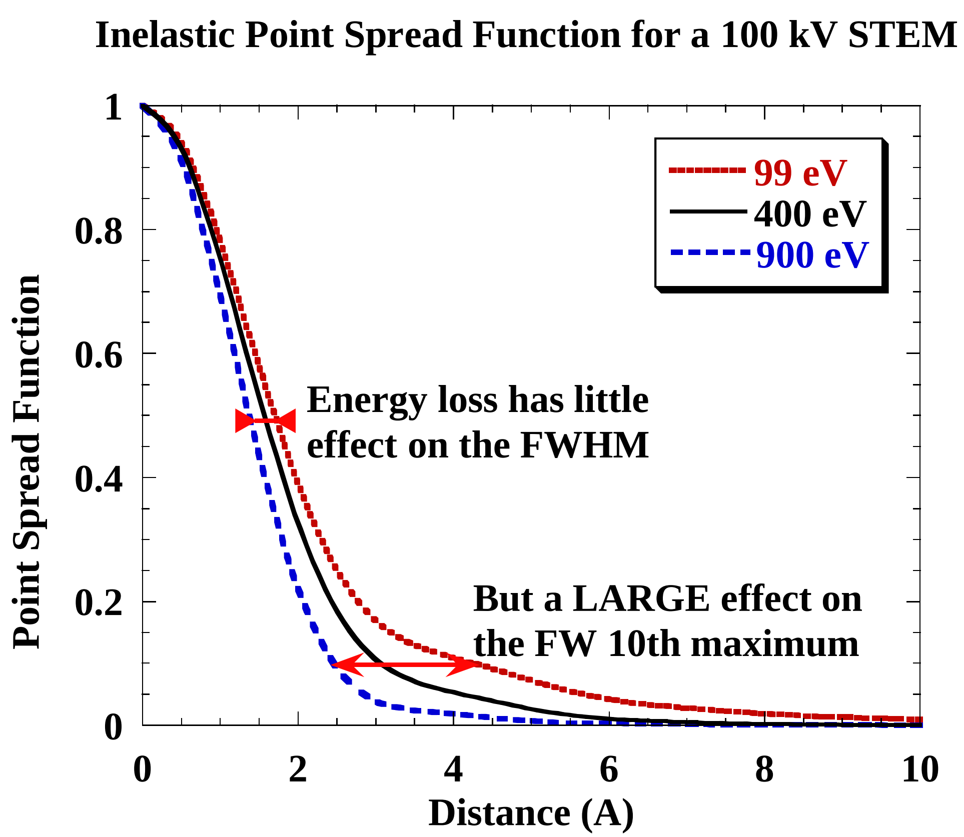

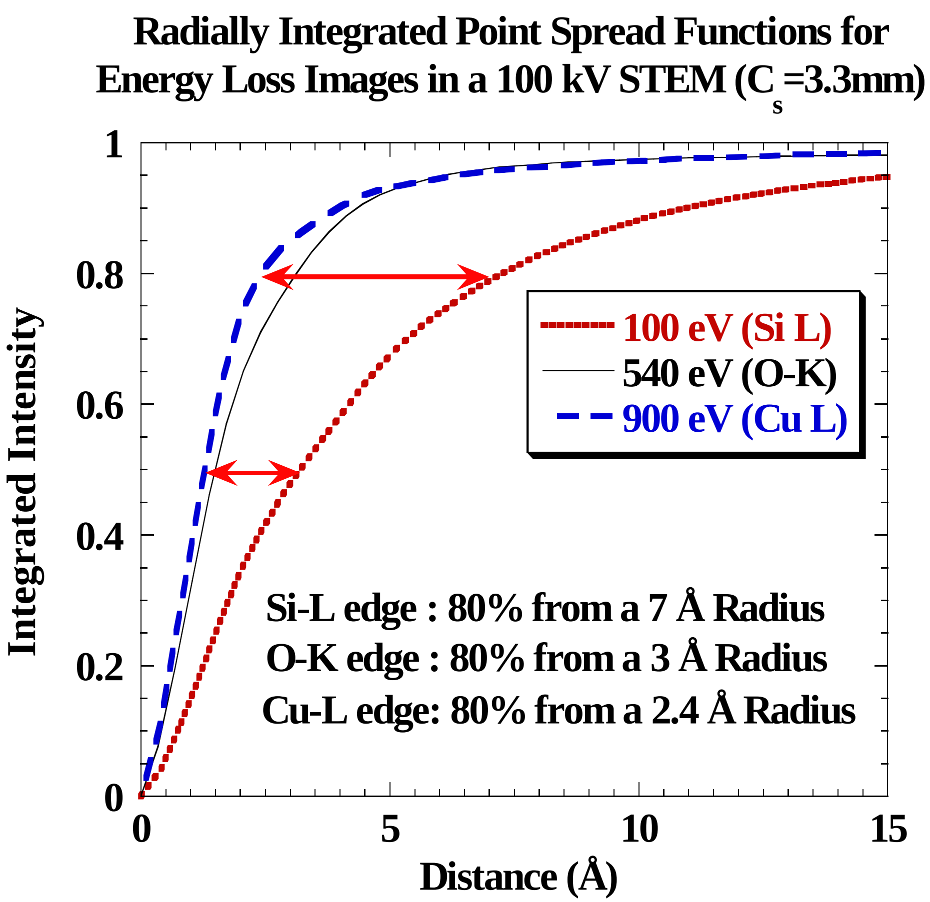

Delocalization has long tails and a sharp central peak

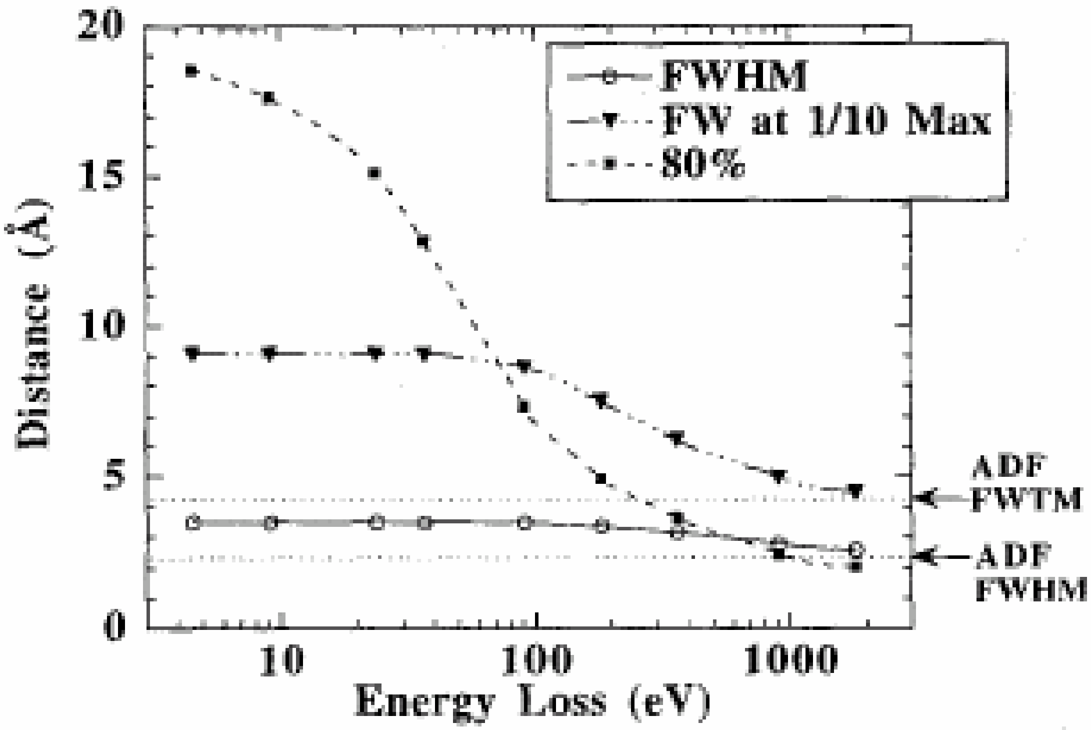

Fig. 8. Measures of spatial resolution for a 100 kV STEM at 1100 Å defocus with $C_s = 3.3$ mm, a 8.18 mrad objective aperture and a 10 mrad collector aperture. The full width at half maximum (FWHM), full width at tenth maximum and the radius of the disk containing 80% of the scattered electrons are shown for $P(b, E)$ from a single dipole, calculated using Eq. (13).

D.A. Muller, J. Silcox / Ultramicroscopy 59 (1995) 195–213

Bulk and Surface Plasmons

Screening inside a solid $\frac{1}{\varepsilon(\omega)}$

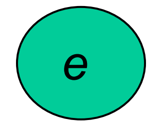

Screening outside e a solid
(screening of the image charge) $\frac{1}{\varepsilon(\omega)+1}$

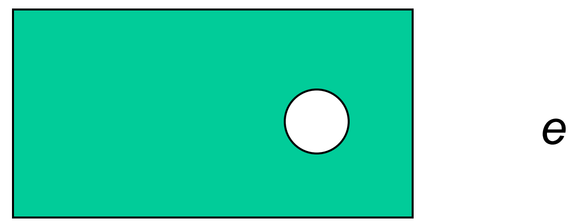

Bulk energy loss: $P(\omega)\,\alpha\,\mathrm{Im}\left(\frac{-1}{\varepsilon(\omega)}\right)$

Plasmon pole ω_p, at ε=0

surface energy loss: $P(\omega)\,\alpha\,\mathrm{Im}\left(\frac{-2}{\varepsilon(\omega)+1}\right)$

Plasmon pole $1/\sqrt{2}\omega_p$, at ε=-1

Plasmons at an interface

A. Howie / Micron 34 (2003) 121–125

Bulk

$$\frac{2\pi^2\varepsilon_0\hbar^2v^2}{e^2}\frac{\mathrm{d}P(b,\omega)}{\mathrm{d}\hbar\omega} = \mathrm{Im}\left\{\frac{-1}{\varepsilon_{\mathrm{B}}(\omega)}\right\}\ln\left(\frac{q_c v}{\omega}\right) + K_0\left(\frac{2\omega b}{v}\right)\left[\mathrm{Im}\left\{\frac{-2}{\varepsilon_{\mathrm{A}}(\omega)+\varepsilon_{\mathrm{B}}(\omega)}\right\} - \mathrm{Im}\left\{\frac{-1}{\varepsilon_{\mathrm{B}}(\omega)}\right\}\right] \quad (1)$$

Interface plasmon

$b_{max}=v/\omega$ *Is the natural length scale Where plasmon effects become noticeable (a few nm for plasmons)*

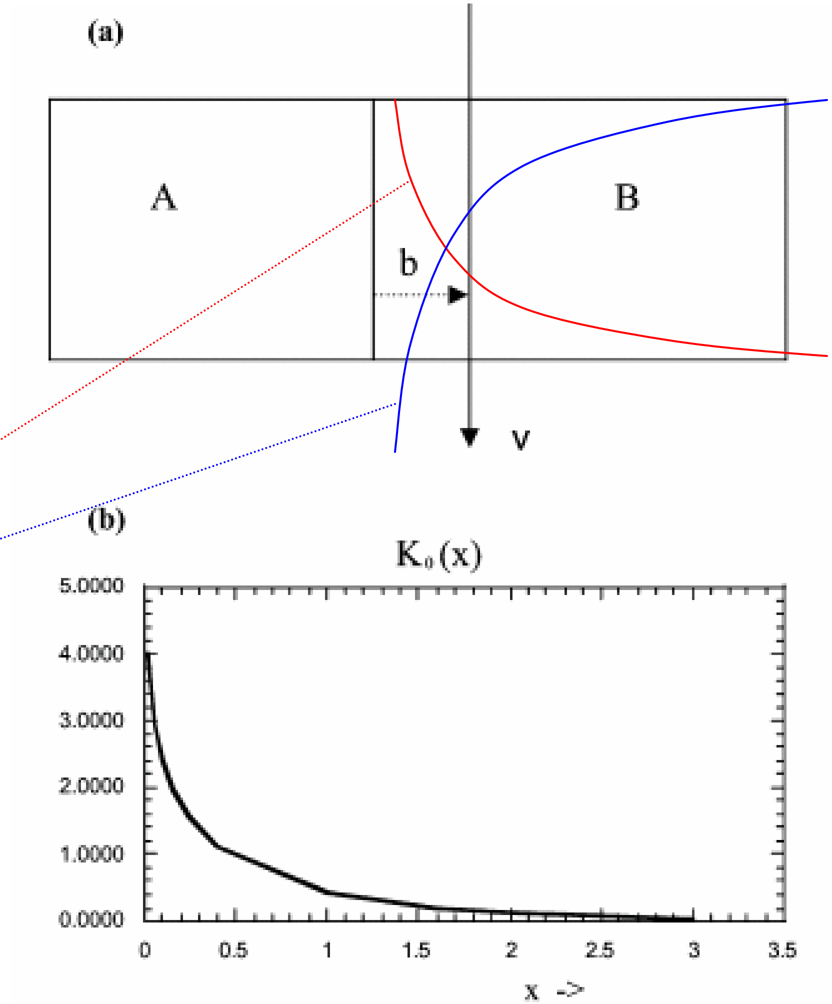

Fig. 1. (a) Typical geometry for the collection of electron energy loss spectra as a function of impact parameter b near a planar interface in a thin film. (b) The function $K_0(x)$ describes the spatial influence of the boundary with $x = 2\omega b/v$.

EELS across a 50 nm thick Silicon edge

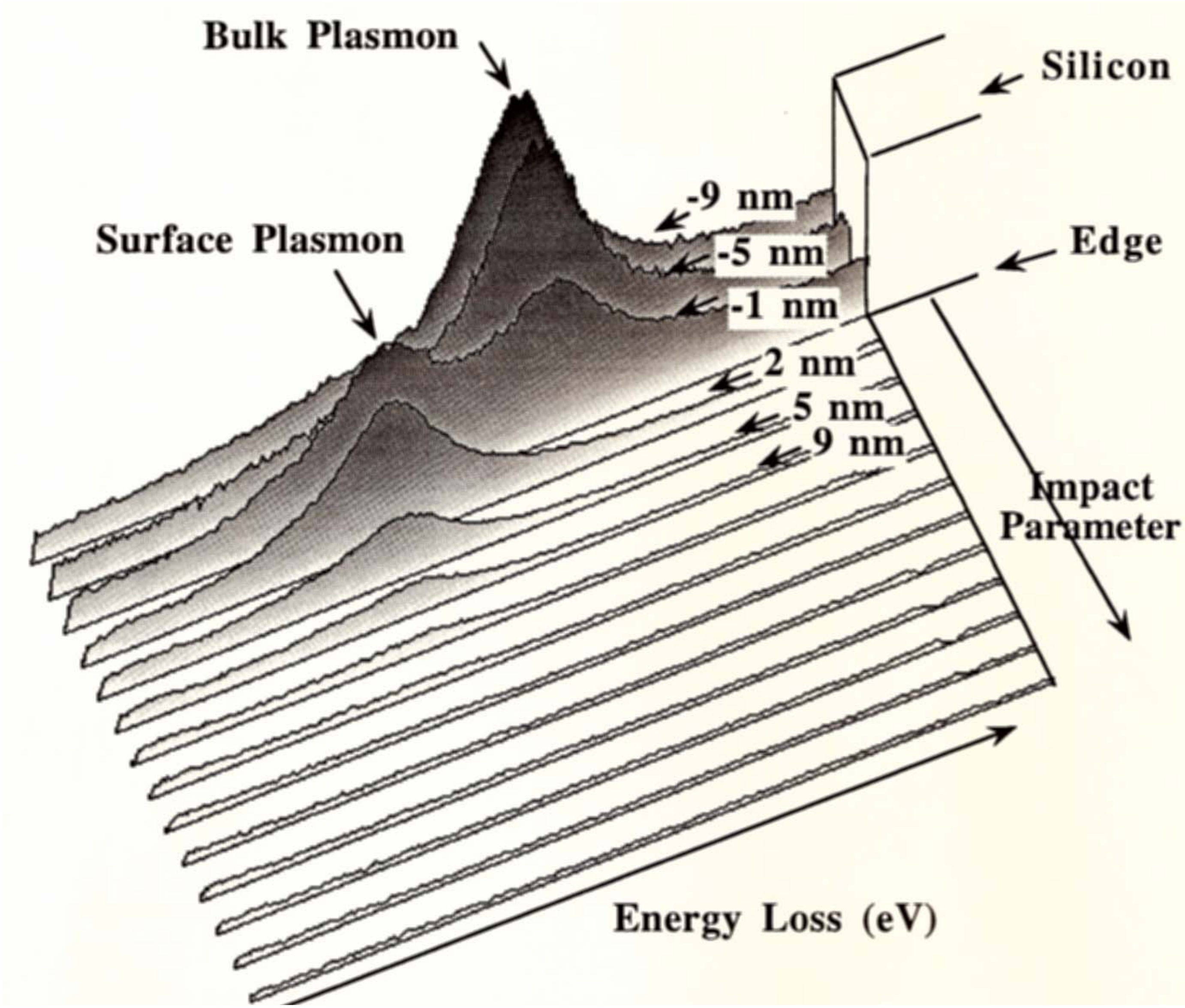

Valence EELS from a thin interlayer?

A. Howie / Micron 34 (2003) 121–125

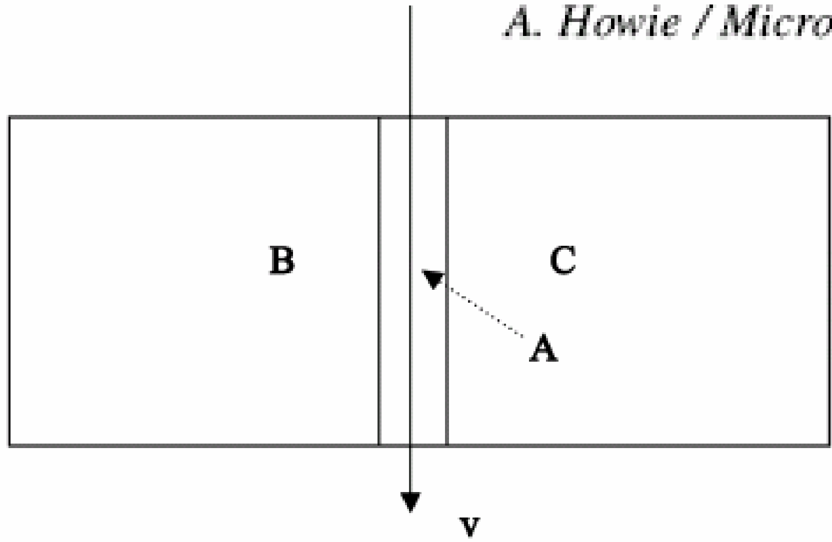

Fig. 2. Dielectric sandwich with a thin boundary phase A separating two other dielectric B and C.

When layer A becomes thinner than $_{x}v/\omega$, the bulk mode from A is suppressed. (i.e. can't measure the bulk dielectric function of a grain boundary phase – must use Interface formula)

e.g. Neyer et al., 1997. Plasmon coupling and finite size effects in metallic mutilayers. *J. Microsc.* **187**, 184–192.

Valence EELS on Nanoparticles

When a nanoparticle is smaller than v/ω, the probe will also excite spherical, multipole plasmon modes.

Spherical CavityModes

$$\omega_{\text{void}} = \left[\frac{l+1}{2l+1} \right]^{1/2} \omega_p \; ,$$

Spherical Modes

$$\omega_s = \left[\frac{l}{2l+1} \right]^{1/2} \omega_p \; .$$

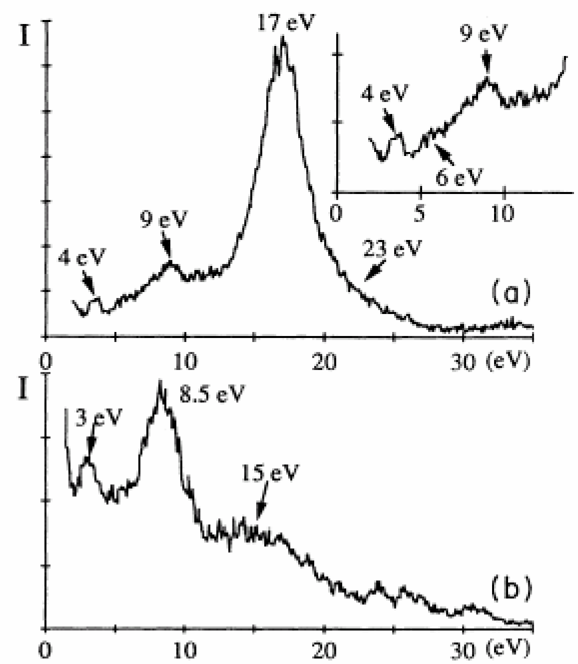

FIG. 2. Typical low-energy-loss spectra of silicon particles: (a) over a particle; (b) grazing incidence.

*D. Ugarte, C. Colliex, P. Trebbia, Phys Rev **B45** (1992) 4332*

Valence EELS on Nanoparticles

Cherenkov Radiation

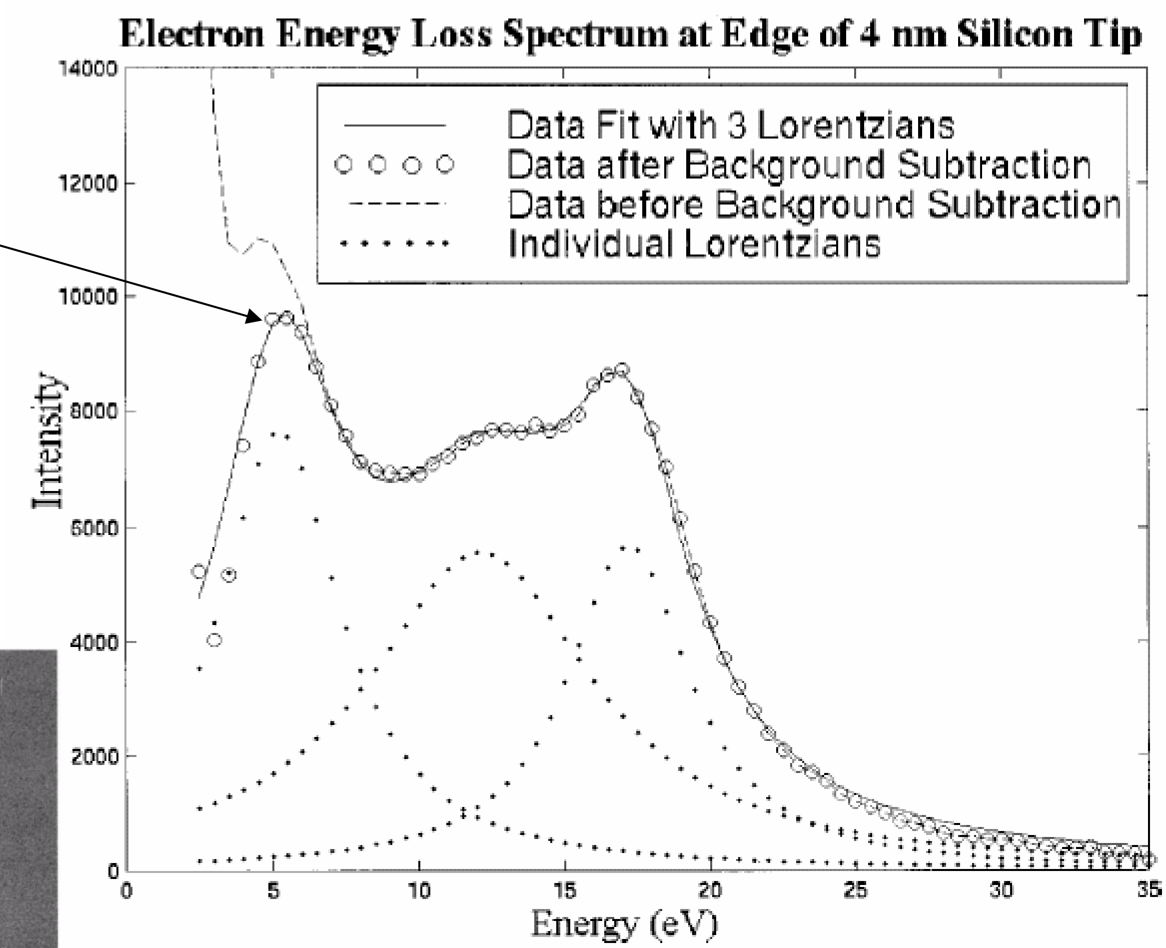

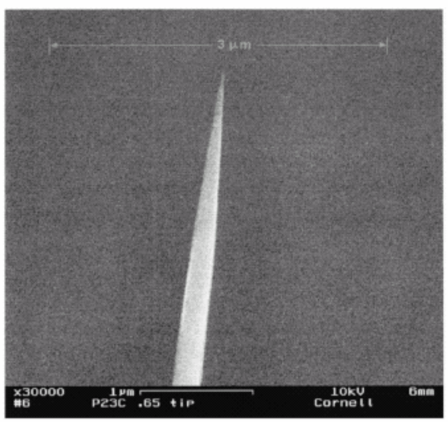

B.W.Reed et al, Phys Rev ***B60*** *(1992) 5641*

Summary

- *The EELS signal is localized to within a few Angstroms for core edges*
- *and on the order of 1-6 nm for valence (1-30 eV) excitations.*

- *Valence EELS on small particles measures more than just the bandgap*
- *Surface plasmons, Cherenkov radiation are just as important*